Pressure Tuned Insulator to Metal Transition in $Eu_2Ir_2O_7$

F. F. Tafti,[1] J. J. Ishikawa,[2] A. McCollam,[3] S. Nakatsuji,[2] and S. R. Julian[1,4]

[1]*The Department of Physics, University of Toronto,*
60 St. George Street, Toronto, Ontario, M5S 1A7, Canada
[2]*Institute for Solid State Physics, University of Tokyo, Kashiwa, Chiba 277-8581, Japan*
[3]*High Field Magnet Laboratory, Institute for Molecules and Materials,*
Radboud University Nijmegen, 6525 ED Nijmegen, The Netherlands
[4]*Canadian Institute for Advanced Research, Quantum Materials Program,*
180 Dundas St. W., Suite 1400, Toronto, ON, Canada M5G 1Z8
(Dated: May 16, 2012)

We have studied the effect of pressure on the pyrochlore iridate $Eu_2Ir_2O_7$, which at ambient pressure has a thermally driven insulator to metal transition at $T_{MI} \sim 120$ K. As a function of pressure the insulating gap closes, apparently continuously, near $P \sim 6$ GPa. However, rather than T_{MI} going to zero as expected, the insulating ground state crosses over to a metallic state with a negative temperature coefficient of resistivity, suggesting that these ground states have a novel character. The high temperature state also crosses over near 6 GPa, from an incoherent to a conventional metal, implying that there is a connection between the high and the low temperature states.

PACS numbers: 71.30.+h, 62.50.-p

INTRODUCTION

Putting itinerant electrons with strong spin-orbit coupling on geometrically frustrated lattices offers new possibilities for strongly correlated electron states. Recent attention has focused on the pyrochlore iridates, $R_2Ir_2O_7$ where R is a rare earth, for which several theoretical studies propose the existence of topologically non-trivial ground-states [1–4]. Testing such predictions requires advanced experiments, for example measurements that can reveal unconventional quantum phase transitions [5]. Here, we report an unusual insulator-to-metal quantum phase transition in the pressure-temperature phase diagram of the pyrochlore iridate $Eu_2Ir_2O_7$.

Amongst pyrochlore oxides, iridates have their M-sites occupied by Ir^{4+} ions whose extended $5d$ orbitals are prone to strong electron-lattice and spin-orbit couplings [6]. Compared with the less extended orbitals of $3d$ transition metal oxides, iridates are naively expected to be less strongly correlated. Nevertheless, the strong spin-orbit and electron-lattice couplings can lift the orbital degeneracy of iridium $5d$ electrons and narrow their bandwidths. Hence iridates can be delicately poised near a bandwidth controlled metal insulator transition (MIT).

Successive replacement of the R site of $R_2Ir_2O_7$ with larger rare earth atoms causes a change from insulating to metallic behaviour [7, 8]. Progressing from right to left in the Lanthanide series, (Lu, Yb, ..., Gd)$_2Ir_2O_7$ are all insulators; (Eu, Sm, and Nd)$_2Ir_2O_7$ are on the boundary, looking metallic at high temperatures but insulating at low temperatures, and $Pr_2Ir_2O_7$ is metallic down to the lowest temperatures. Increasing the R size in the $R_2Ir_2O_7$ series makes the Ir-O-Ir bond angle wider and the Ir-O bond length shorter. As a result, the iridium t_{2g} bandwidth increases and eventually passes the metallization threshold beyond a certain R ionic radius [9].

As the R size increases from Eu to Nd, (Eu, Sm, and Nd)$_2Ir_2O_7$ show several signatures of a weakening low-temperature insulating phase and a strengthening high-temperature metallic phase [8]: (1) the metal-insulator transition temperature T_{MI} is significantly smaller in the Nd compound (36 K) compared to the Eu and Sm compounds (120 and 117 K respectively); (2) the small and temperature dependent gap ($\Delta < 10$ meV) of the insulating phase is smallest in the Nd compound [8]; (3) the Nd compound has the smallest inverse RRR ratio defined as R_{4K}/R_{300K}; and (4) in the high temperature metallic phase only the resistivity of the Nd compound is 'metallic', having a positive slope for $\rho(T)$; in Eu and Sm $\rho(T)$ is 'non-metallic', with a weakly negative slope. (By 'non-metallic' we mean a resistivity that rises with decreasing temperature, but with power-law temperature dependence as opposed to the exponential temperature dependence of a gapped insulator.)

These three systems are of particular interest at present, because it is believed that states near the metal-insulator boundary in the pyrochlore iridates may have a toplogical nature [1–4]. In particular, Wan et al. [2] and Witczack-Krempa et al. [3] predict that a toplogical semi-metallic state separates the insulating and the metallic ground states. This 'Weyl semi-metal' is a three-dimensional analogue of graphene, with the chemical potential pinned to Dirac points of chiral states. In order to form, the Weyl semi-metallic state requires magnetic order, and due to the vanishing density of states at the chemical potential, the electrical conductivity of the bulk is predicted to vanish when $T \to 0$ K [2, 4, 10].

Electron interactions and correlations of pyrochlore iridates can be tuned by either chemical or physical pressure. For investigating the nature of the low tempera-
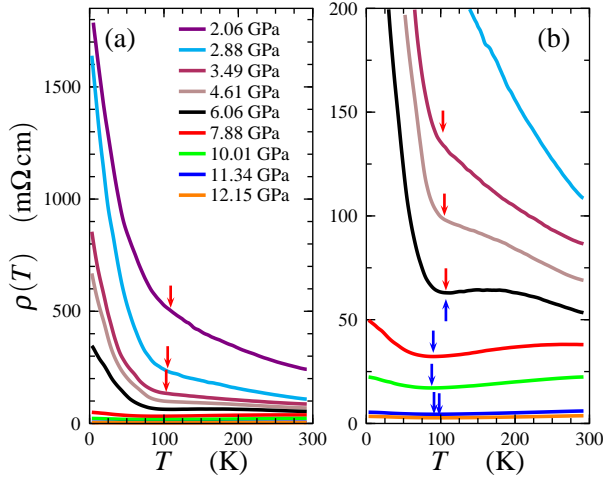
FIG. 1. Resistivity as a function of temperature from $P = 2.06$ to $12.15\,\mathrm{GPa}$. The left-hand panel contains all of our results, showing that the resistivity is strongly suppressed by increasing pressure. The right-hand panel focuses on the intermediate-pressure data. Red arrows indicate the metal-insulator transition (see Fig. 2 and the text); blue arrows indicate the minimum in $\rho(T)$.

FIG. 2. Locating the metal-insulator transition, T_{MI}. The color coding is the same as in Fig. 1. The transition does not have a strong signature in $\rho(T)$, however panel (a) shows that there is a marked change in slope of $\log(\rho)$ vs. T near 100 K at all pressures, while panel (b) shows that the onset of this behaviour can be found, for all pressures below 7.88 GPa, in a sharp downturn in $\partial\rho/\partial T$. As a guide to the eye we have shown plausible extrapolations of the high-temperature slope, and the slope immediately below 100 K. At each pressure we have placed T_{MI} at the mid-point between the onset of the downturn and the temperature at which the these extrapolations meet; while the error bars (see Fig. 4) extend to these two temperatures. The inset of (b) zooms in on $\partial\rho/\partial T$ near 100 K for 3.49 GPa. In (a) some curves are offset vertically for clarity.

ture state, physical pressure has the obvious advantage that it can be tuned continuously. (Continuous substitution studies in the pyrochlore iridates are not useful, since the ground state is sensitive to disorder [8].) Physical pressure is somewhat different from chemical pressure, however. Increasing the R atomic size increases the Ir-O-Ir bond angle and the lattice parameter in parallel [7], while hydrostatic pressure increases the former but decreases the latter. Thus we expect new insights from the application of physical pressure to explore the boundary between metallic and insulating ground states in pyrochlore iridates.

EXPERIMENT

Eu$_2$Ir$_2$O$_7$ single crystals were grown at ISSP using the KF-flux method [11]. We pressurized samples measuring approximately $150 \times 100 \times 30~\mu\mathrm{m}^3$ in a moissanite anvil cell [12] and measured resistivity as a function of temperature at several pressures in the range P = 2 to $12\,\mathrm{GPa}$, using a four terminal ac method. The pressure medium was 7373 Daphne oil, and pressure was monitored by ruby fluorescence spectroscopy at room temperature. A 1 K dipping probe was used in the temperature range T = 300 to 2 K. Resistivity below 2 K and magnetoresistance at 10.01 GPa were measured in a dilution refrigerator.

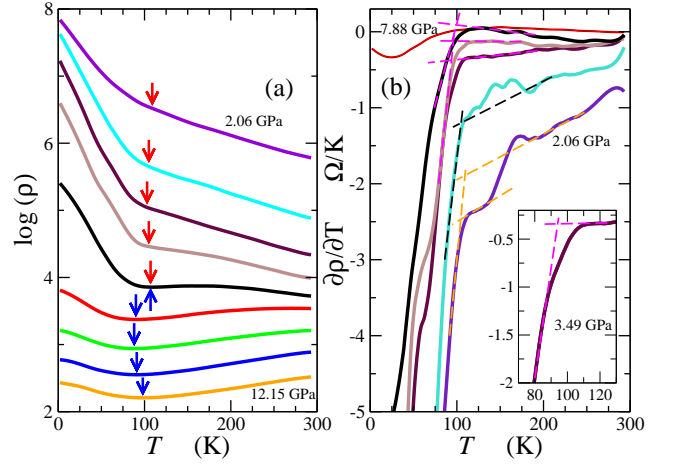## RESULTS

Our resistivity data, from 300 to 2 K at nine different pressures from 2.06 to 12.15 GPa, are presented in Fig. 1. The quantitative effects of increasing the pressure from 2 to 12 GPa are dramatic: the room temperature resistivity falls by a factor of 60, while the 2 K resistivity falls by a factor of 500. Qualitatively, the slope of the resistivity, $\partial\rho(T)/\partial T$, for $T > 100$ K changes from negative (non-metallic) at low pressure to positive (metallic) at 10 and 12 GPa. At lower temperature, in contrast, the slope of the resistivity is negative at all pressures, but it is nearly 1000 times larger at 2.06 GPa than at 12.15 GPa. We elaborate on the low temperature resistivity in the Discussion, and show that the low pressure curves have a temperature dependent gap that closes between 6 and 8 GPa.

The metal-insulator transition, which occurs at 120 K at ambient pressure, does not show up clearly in the raw resistivity. This is also the case at ambient pressure [8]. However, Fig. 2 shows that, for low pressures, the slope of $\log(\rho(T))$ vs T changes near 100 K. This change appears to be quite abrupt in the 3.49 GPa and the 4.61 GPa curves, both in Fig. 2(a) and in the raw data (Fig. 1(b)). This change in slope is more clearly seen in plots of
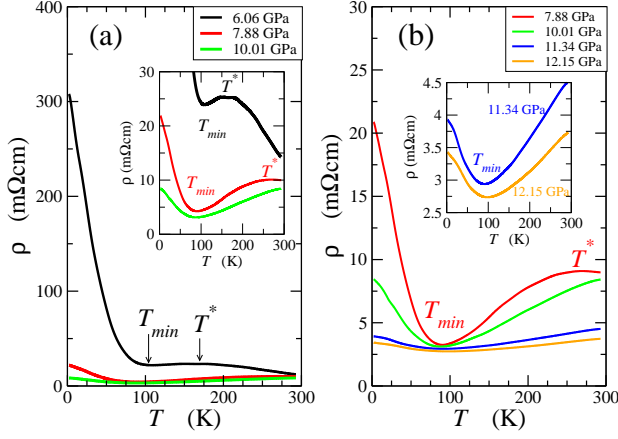
FIG. 3. Location of T^* and T_{min}. The main panel in (a) shows $\rho(T)$ from 6.06 to 10.01 GPa, while the inset shows an expanded view around T^* and T_{min}. The curves are offset vertically to give a better view of the data. The main panel in (b) shows $\rho(T)$ from 7.88 to 12.15 GPa. The inset is an expanded view of the two highest pressure curves with $RRR < 1$.

$\partial\rho/\partial T$ vs. T (Fig. 2(b)): for all pressures below 7.88 GPa, $\partial\rho/\partial T$ begins to decrease rapidly, with a sharp, well-defined onset, near 100 K. We have used this to identify T_{MI}: down to T_{MI} the slope of $\partial\rho/\partial T$ is roughly constant, then at T_{MI} it begins to fall rapidly. The inset of Fig. 2(b) shows a clear example, at 3.49 GPa. The red arrows in the first two figures correspond to T_{MI}, assigned to the mid-point between where the slope first starts to turn downwards, and the point where the extrapolated high and low temperature slopes meet. Error bars on our phase diagram, discussed below, extend to these two temperatures. The lowest pressure $\partial\rho/\partial T$ curves are rather noisy, perhaps because the contact resistances, which improved as the pressure increased, were rather large, but even in these cases a sharp change can be identified quite accurately.

At 6.06 GPa and above, there is a minimum in $\rho(T)$, and like T_{MI} it is close to 100 K. The way this minimum develops is shown in Fig. 3. In the lower pressure curves the resistivity has a negative slope at all temperatures, but in the 6.06 and 7.88 GPa curves an intemediate region of $\partial\rho/\partial T > 0$ develops below a local maximum at T^* and a local minimum at T_{min}. At higher pressure the maximum has apparently moved above room temperature, so $\rho(T)$ has a positive, metallic, slope from T_{min} to 293 K. The T^* cross-over occurs at 180 and 270 K on the $P = 6.06$ and 7.88 GPa curves respectively.

We have used the qualitatively different resistivity behaviours to construct a phase diagram, shown in Fig. 4. The phase diagram can be viewed as four quadrants, corresponding to four distinct regimes of electronic transport. In the top left quadrant ($P \lesssim 6$ GPa, $T \gtrsim 100$ K), the system is an "incoherent metal" characterized by a
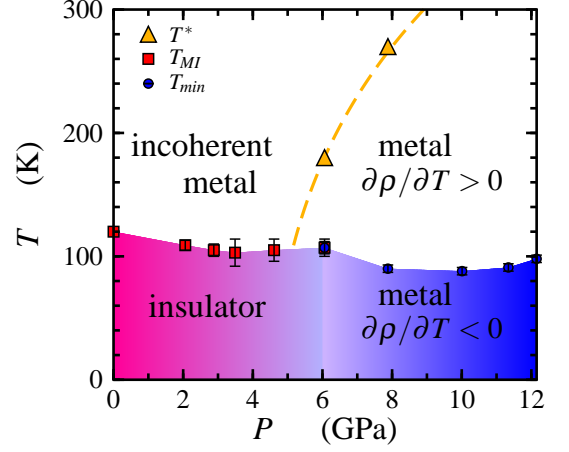

FIG. 4. The phase diagram for $Eu_2Ir_2O_7$ constructed from our resistivity data. At low pressures, $P < 6$ GPa, the finite temperature MIT is indicated by red squares; the value at 0 GPa is taken from reference [8]. At high pressures, $P > 6$ GPa, the transition between conventional and negative-$\partial\rho/\partial T$ metallic states is indicated by blue circles. The T^* cross-over is shown by orange triangles. All the lines are guides to the eye. The quantum critical point (QCP) separating the insulating and the negative $\partial\rho/\partial T$ metal lies on the P axis near $P_c = 6.06 \pm 0.60$ GPa. Both T_{MI} and T_{min} depend weakly on T.

high resitivity and a power-law temperature dependence with a non-metallic slope, $\partial\rho(T)/\partial T < 0$. The MIT at T_{MI} separates the incoherent metallic phase from the "insulating" phase in the bottom left quadrant ($P \lesssim 6$ GPa, $T \lesssim 100$ K), characterized by an exponentially activated resistivity, as discussed below.

In the top-right quadrant ($P \gtrsim 6$ GPa, $T \gtrsim 100$ K), the system is a "conventional metal" characterized by a metallic slope, $\partial\rho(T)/\partial T > 0$. The cross-over at T_{min} separates the conventional metal and the "negative $\partial\rho(T)/\partial T$ metal" ($P \gtrsim 6$ GPa, $T \lesssim 100$ K), whose resistivity increases with decreasing temperature in a non-Fermi liquid (NFL) power-law fashion (Fig. 3(b)).

The two high-temperature regimes, the conventional metal and incoherent metal, are separated by the T^* cross-over, at which the slope of $\rho(T)$ changes from positive to negative.

We distinguish between the incoherent metal (in the top-left quadrant) and the negative $\partial\rho/\partial T$ metal (in the bottom right-quadrant). Although they both have power-law dependence on T with negative $\partial\rho/\partial T$, their absolute resitivities differ by a factor of up to 500, and the latter probably has Landau-type quasiparticles as established by the metallic resistivity at high temperature, while in the incoherent metallic phase it is likely that quasiparticles have not formed.

This phase diagram is in broad agreement with the effects of chemical pressure [8], but with the clear difference that T_{MI} changes rapidly with chemical pressure, falling

from 201 K to 36 K in going from $Eu_2Ir_2O_7$ to $Nd_2Ir_2O_7$, while in our measurements it is nearly pressure independent. Moreover, T^* is not seen in the chemical pressure measurements.

Our phase diagram suggests a connection between the high and low temperature phases of $Eu_2Ir_2O_7$: the incoherent metal becomes insulating below T_{MI}; the conventional metal crosses over to the negative $\partial\rho/\partial T$ metal below T_{min}; in other words the transition between the insulating and the negative $\partial\rho/\partial T$ metallic ground states at $P_c = 6.06 \pm 0.60$ GPa coincides with the incoherent-coherent cross-over at $T^* > 100$ K.

DISCUSSION

To discuss our results, we start with the high temperature part of the phase diagram. The incoherent metallic phase is characterized by a high resistivity and a negative $\partial\rho(T)/\partial T$ that are both gradually suppressed by increasing pressure. Metallic phases in the vicinity of localization transitions are usually subject to strong fluctuations in the spin, charge and orbital degrees of freedom, resulting in unconventional transport properties. The negative $\rho(T)$ slope in the incoherent metallic regime of $Eu_2Ir_2O_7$ is probably an example of such physics.

The boundary between the two high temperature regimes is marked by the dashed T^* line in Fig. 4. The broad peaks at T^* (Fig. 3) mark a coherent-incoherent cross-over of the quasiparticle dynamics that is also typical of correlated oxides in proximity to a Mott transition [13, 14]. The T^* cross-over has not been observed in the previous chemical pressure measurements in pyrochlore iridates by replacing the R site with larger atoms: it presumably takes place somewhere between $Sm_2Ir_2O_7$ and $Nd_2Ir_2O_7$. Moreover, it probably cannot be realized by alloying on the R site, i.e. partially replacing Eu or Sm with Nd, because of the extreme sensitivity of these systems to disorder [8]. Physical pressure is therefore the only means by which T^* can be observed.

A similar pressure-induced coherent-incoherent cross-over has been observed in $Gd_2Mo_2O_7$, which is located at the boundary between a FM metal and a spin glass Mott insulator in the $R_2Mo_2O_7$ series [15]. $Gd_2Mo_2O_7$ goes through a continuous bandwidth-controlled insulator to metal quantum phase transition at $P_c = 2.4$ GPa [16]. Simultaneously a cross-over appears at $T^* \approx 150$ K in the resistivity data. T^* shows a strong pressure dependence in both $Eu_2Ir_2O_7$ (Fig. 4) and $Gd_2Mo_2O_7$ [15]: T^* shifts at a rate $\Delta T^*/\Delta P \sim 50$ K/GPa in $Eu_2Ir_2O_7$ and ~ 35 K/GPa in $Gd_2Mo_2O_7$.

Turning now to the low temperature part of the phase diagram, previous studies [8] have treated the low temperature regimes of $Eu_2Ir_2O_7$, $Sm_2Ir_2O_7$ and $Nd_2Ir_2O_7$ as a Mott insulating phase with a so-called temperature dependent gap (a gap that gets smaller with decreasing
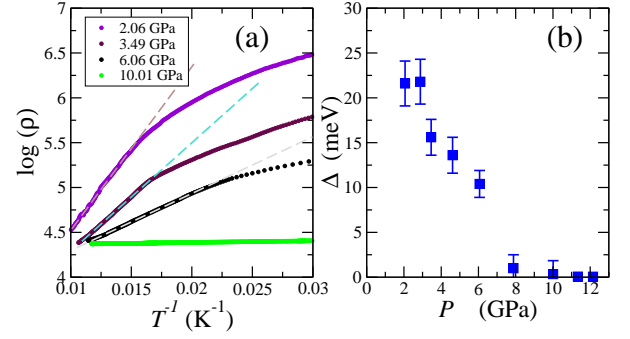

FIG. 5. (a) $\log(\rho(T))$ vs. $1/T$ at selected pressures between 100 K and 30 K. The gap, $\Delta(P)$, is extracted by fitting a single exponential to the resistivity data at each pressure in the temperature range 60 K $\leq T < T_{MI}$ (dashed lines). These curves have been shifted vertically to allow easier comparison of the slopes. (b) The maximum value of the gap $\Delta(P)$, extracted as shown in figure (a), is continuously suppressed by pressure.
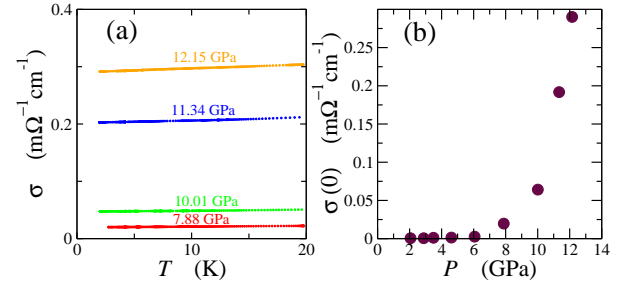

FIG. 6. (a) The conductivity $\sigma(T)$ below 20 K. The data were extrapololated to 0 K to get the residual conductivity values plotted in (b). (b) The residual conductivity plotted as a function of pressure, indicating that the pressure induced insulator to metal quantum phase transition is continuous.

T, with a non-divegent resistivity in the $T \to 0$ K limit). In all three systems there is a magnetic anomaly at the metal-insulator transition [8, 17, 18]. Unlike the Sm and Nd systems, however, $Eu_2Ir_2O_7$ does not show a sharp metal-insulator transition in the resistivity, rather there is a rapid cross-over from power-law resistivity at high temperature to thermally activated behaviour below the 120 K magnetic transition. We do not yet have magnetic data at high pressure, which would allow us to unambiguously determine T_{MI}, however the clear signatures in $\partial\rho/\partial T$ and in $\log(\rho)$ vs. T (Fig. 2), which connect smoothly to 120 K at ambient pressure (Fig. 4) give us confidence that we can identify T_{MI}.

This is further reinforced by plots of $\log(\rho)$ vs. $1/T$, in Fig. 5(a), which have a straight-line dependence for a significant range of temperature below T_{MI} as expected for a gapped system. If we plot the gap extracted from this straight line behaviour as a function of pressure then the gap appears to vanish continuously between 6 and 8 GPa (Fig. 5(b)). Similarly, if we plot the $T = 0$ K conductiv-

ity, $\sigma(0)$, obtained by extrapolating our resistivity curves to 0 K (Fig. 6) the conductivity appears to rise continuously across this pressure range. These behaviours are consistent with a Mott insulating ground state at low pressure followed by a continuous insulator-to-metal transition between 6 and 8 GPa. In this scenario, the non-divergence of the resistivity as $T \to 0$ K may be due to bulk impurity states. Indeed, $\rho(0)$ shows a strong sample dependence, consistent with impurity states in the bulk. However the role of disorder in the insulating phase is not clear, and it should be noted that the MIT at T_{MI} cannot be simple disorder driven Anderson localization, because disorder wipes out the insulating phase and leaves the system metallic at all temperatures [8]. Given the presence of spin 1/2 moments on the iridium sites, frustration-induced localization [19] may play a role in the insulating state, while the recent revelation of a commensurate AFM order in $Eu_2Ir_2O_7$ below 120 K from μSR measurements raises the possibility of gapping of the Fermi surface by a Slater transition [17].

A difficulty with the simple Mott insulator interpretation of our phase diagram is that, although the gap closes continuously with pressure, T_{MI} does not vanish, indeed it is barely affected by pressure (Figs. 4 and 5). It is therefore interesting that recent theoretical proposals, based on band-structure and many-body calculations, have variously proposed strong toplogical insulator ground states [1, 20, 21] and Weyl semi-metallic ground states on the boundary of the metal-insulator transition [2–4] in pyrochlore iridates. These suggestions are consistent with our results. Firstly, the finite resistivity at $T \to 0$ K could arise from small intrinsic Fermi pockets or surface states characteristic of topological insulators. Moreover, Hosur et al. [4] show calculated resistivity for the Weyl semi-metal that agrees qualitatively with our data. Indeed, the fact that T_{MI} is not affected by pressure, while the gap vanishes and residual conductivity rises continuously across the critical pressure, could be explained if T_{MI} is produced by a magnetic transition of the itinerant Ir $5d$-electrons (note that, according to crystal field calculations, Eu has no magnetic moment in this material) that is only weakly pressure dependent, while the underlying electronic structure undergoes (for example) a Lifshitz transition.

We note that our finding of a roughly pressure independent T_{MI} is in contrast to a recent pressure study of $Nd_2Ir_2O_7$ [22] which observed a monotonic suppression of T_{MI} with increasing pressure. We do not have an explanation for this discrepancy. Aside from the different materials, the only obvious difference between the measurements is that the $Nd_2Ir_2O_7$ study used NaCl as the pressure medium, which could produce anisotropic pressures which can have unpredictable effects on geometrically frustrated systems. (In this respect Daphne oil, which we used, is an improvement on NaCl but still
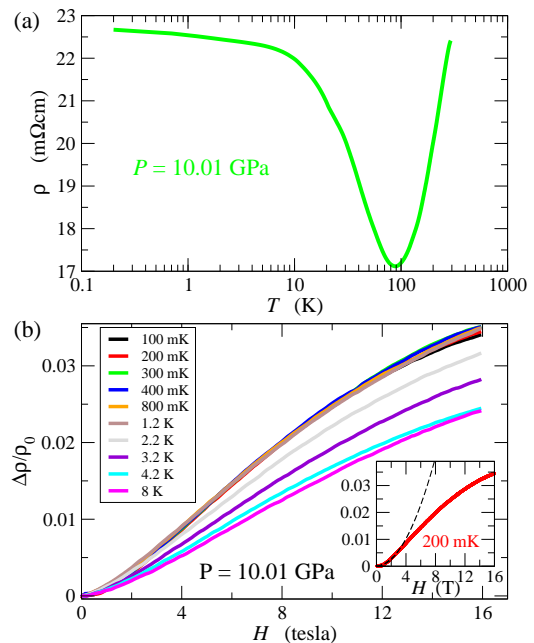

FIG. 7. (a) Semi-logarithmic plot of resistivity from room temperature to 200 mK at $P = 10.01$ GPa. (b) Magnetoresistance as a function of magnetic field at $P = 10.01$ GPa. Data were taken in a temperature range from 100 mK to 8 K. MR is suppressed by increasing temperature. The inset shows a quadratic fit (black dashed line, $M \propto H^2$) to the low field data at $T = 200$ mK. At high fields, MR tends towards saturation.

not ideal at high pressures.)

After the collapse of the insulating phase above 6.06 GPa ($\Delta = 0$, $\sigma(0) \neq 0$), a low-temperature NFL power law rise of resistivity survives up to the highest pressure in our experiment, in the negative $\partial\rho/\partial T$ metal region in the bottom-right quadrant of our phase diagram. The nature of this phase is not clear. Figure 7(a) is a semi-logarithmic plot of $\rho(T)$ at $P = 10.01$ GPa from $T = 300$ K to 100 mK. The NFL resistivity behaviour fits to $\rho(T) = \rho(0) - AT^x$ with $x = 1.0 \pm 0.1$ below 20 K for $P > 6$ GPa. While the resistivity upturn of the metallic phase below T_{min} looks Kondo-like, similar to what is observed in the frustrated Kondo lattice of $Pr_2Ir_2O_7$ [23], crystal-field analyses that predict no local f moments in $Eu_2Ir_2O_7$ [24] would seem to rule out a Kondo effect. Similarly, recent theoretical work [25] that ascribes the resistive upturn in $Pr_2Ir_2O_7$ and in $Nd_2Ir_2O_7$ at high pressure [22] to frustrated spin-ice-like correlations among the local f-electrons, would also appear to be ruled out by the absence of f-moments on the Eu sites.

As well as being a common feature of the metallic pyrochlore iridates, a rising resistivity as $T \to 0$ K has also been observed in metallic pyrochlore molybdates at high pressures. Hydrostatic pressure destroys the FM order in the metallic ground states of (Nd and Sm)$_2$Mo$_2$O$_7$ by tuning the relative strength of double and super-

exchange interactions amongst Mo d electrons. The resulting order-disorder transition coincides with a change in the resistivity behaviour, from conventional metallic to a "diffusive" NFL state [26] characterized by a large, relatively weakly T dependent resistivity, not unlike the resistivity of our $\partial\rho/\partial T > 0$ metal, and also having an upturn in the resistivity as $T \to 0$ K. In this context, it seems significant that the tetragonal antiferromagnet Ba_2IrO_4 [27] has recently been shown to have a continuous pressure-induced insulator-to-metal transition that is related to suppression of magnetism, but in this case the low temperature resistivity at high pressure is metallic. Thus, the upturn in $\rho(T)$ as $T \to 0$ K is not a generic feature of iridates near the boundary of a Mott insulating ground state, rather the pyrochlore lattice structure seems to play a decisive role.

To further investigate the negative $\partial\rho/\partial T$ metallic phase, we measured magnetoresistance (MR) at P = 10.01 GPa by sweeping magnetic field from 0 to 16 tesla at ten different temperatures from 100 mK to 8 K (Fig. 7). The MR signal is positive, which rules out weak localization as the cause of the low temperature upturn in $\rho(T)$, as had been suggested in the molybdates [26]. It probably also rules out other mechanisms involving scattering from spins [25], and indeed it may constrain the possible magnetic order on the Ir sublattice. According to reference [2], if the Ir moments are ferromagnetically aligned the ground state will be metallic; FM metals usually have a negative MR however[28], in contrast to our observations of a positive signal. So our results suggest that the ground state is either antiferromagnetic or has the so-called "all-in/all-out" configuration of spins on each Ir tetrahedron. According to references [2, 3], these magnetic configurations could have a Weyl semi-metallic phase separating the Mott insulating and the metallic ground states.

The weak positive MR signal grows quadratically at low fields ($M \propto H^2$), tends towards saturation at high fields, and becomes smaller with increasing temperature. Such behaviour is generic to (non-ferromagnetic) metals with closed orbits on the Fermi surface [28]. The weakness of the MR signal (Fig. 7) may be due to strong scattering, otherwise a state with small pockets should have large MR due to the small Fermi volume and the low density of carriers. The origin of such strong scattering is not clear, although it is consistent with the fairly large resistivity of these samples, even in the metallic regime; moreover the metallic state must be unconventional due to the non-metallic slope of the resistivity $\partial\rho/\partial T < 0$, and the non-Fermi-liquid power-law T dependence.

Further measurements are urgently required in order to elucidate the nature of the negative $\partial\rho/\partial T$ metallic phase. For example, reference [2] predicts that the all in/out spin configuration on the Ir tetrahedra has a 1.3 meV gap to the collinear ferromagnetic state. With this gap, our maximum field of 16 T could be sufficient to cause a reorientation of the spins to ferromagnetic, which would cause a huge jump in magnetoresistance, which we do not observe. However, depending on the accuracy of that calculation, a higher magnetic field may be required, so higher field measurements would be informative.

CONCLUSION

Using resistivity, we have mapped the temperature-pressure phase diagram of $Eu_2Ir_2O_7$ between 2 and 12 GPa. The metal-insulator boundary is near 6 GPa. At high temperature ($T > 100$ K), the resistivity falls by a factor of more than 60 between 2 and 12 GPa, and the behaviour crosses over near 6 GPa from an incoherent metal with a very high resistivity and a negative $\partial\rho/\partial T$, to a more conventional metal having a positive $\partial\rho/\partial T$. At intermediate pressures the cross-over is observed as a function of temperature: the sign of $\partial\rho/\partial T$ changes from positive to negative at a temperature T^* that was not observed using chemical pressure.

The low temperature behaviour evolves from a low pressure "insulating" state, having a temperature dependent gap but a resistivity that does not diverge as $T \to 0$ K, to an anomalous metallic state again having a negative $\partial\rho/\partial T$. Conventional explanations for this rising resistivity as $T \to 0$ K, such as the Kondo effect or weak localization, are ruled out. The transition between these ground states is continuous, with the critical pressure near 6 GPa, however there is no temperature scale apparent in the resistivity that vanishes at the critical pressure, rather the high-to-low temperature cross-over persists across the entire phase diagram. An obvious scenario is that the low-temperature phases occur below a magnetic phase transition that is essentially unaffected by pressure.

The high absolute value and the low temperature rise of the resistivity in the negative $\partial\rho/\partial T$ metallic phase of $Eu_2Ir_2O_7$ might be manifestations of a topological semimetallic phase. The anomalous nature of the ground states on both sides of the QCP suggests a topological character for the quantum phase transition and may explain its unusual form. These results should encourage further experiments to test for the existence of topological states near the metal-insulator boundary of the pyrochlore iridates.

[1] D. Pesin and L. Balents, Nat. Phys. **6**, 376 (2010).

[2] X. Wan, A. M. Turner, A. Vishwanath, and S. Y. Savrasov, Phys. Rev. B. **83**, 205101 (2011).

[3] W. Witczak-Krempa and Y. B. Kim, arXiv:cond-mat/1105.6108 (2011).

[4] P. Hosur, S. A. Parameswaran, and A. Vishwanath, arXiv:cond-mat/1109.6330 (2011).

[5] S. Tewari, J. D. Sau, V. W. Scarola, C. Zhang, and S. D. Sarma, arXiv:cond-mat/1106.5506 (2011).

[6] O. B. Korneta, S. Chikara, S. Parkin, L. E. DeLong, P. Schlottman, and G. Cao, Phys. Rev. B **81**, 045101 (2010).

[7] D. Yanagashima and Y. Maeno, J. Phys. Soc. Jpn. **70**, 2880 (2001).

[8] K. Matsuhira, M. Wakeshima, R. Nakanishi, Y. Yamada, A. Nakamura, W. Kawano, S. Takagi, and Y. Hinatsu, J. Phys. Soc. Jpn. **76**, 043706 (2007).

[9] H. J. Koo and M. H. Whangbo, J. Solid. St. Chem. **136**, 269 (1998).

[10] L. Balents, Physics **4**, 36 (2011).

[11] J. N. Millican, R. T. Macaluso, S. Makatsuji, Y. Machida, Y. Maeno, and J. Y. Chan, Matt. Res. Bull. **42**, 928 (2007).

[12] J. Xu and H. Mao, Science **290**, 783 (2000).

[13] I. Kézsmárki, N. Hanasaki, D. Hashimoto, S. Iguchi, Y. Taguchi, S. Miyasaka, and Y. Tokura, Phys. Rev. Lett. **93**, 266401 (2004).

[14] A. Georges, G. Kotliar, W. Krauth, and M. J. Rozenberg, Rev. Mod. Phys. **68**, 13 (1996).

[15] N. Hanasaki, M. Kinuhara, I. Kezsmarki, S. Iguchi, S. Miyasaka, N. Takeshita, C. Terakura, H. Takagi, and Y. Tokura, Phys. Rev. Lett. **96**, 116403 (2006).

[16] Y. Moritomo, S. Xu, A. Machida, T. Katsufuji, E. Nishibori, M. Takata, M. Sakata, and S. W. Cheong, Phys. Rev. B **63**, 144425 (2001).

[17] S. Zhao, J. M. Mackie, D. E. MacLaughlin, O. O. Bernal, J. J. Ishikawa, Y. Ohta, and S. Nakatsuji, Phys. Rev. B **83**, 180402 (2011).

[18] M. W. N. Taira and Y. Hinatsu, J. Phys. Cond. Matt. **13**, 5527 (2001).

[19] D. L. Bergman, W. Congjun, and L. Balents, Phys. Rev. B. **78**, 125104 (2008).

[20] B. J. Yang and Y. B. Kim, Phys. Rev. B. **82**, 085111 (2010).

[21] M. Kargarian, J. Wen, and G. A. Fiete, Phys. Rev. B. **83**, 165112 (2011).

[22] M. Sakata, T. Kagayama, K. Shimizu, K. Matsuhira, S. Takagi, M. Wakeshima, and Y. Hinatsu, Phys. Rev. B **83**, 041102(R) (2011).

[23] S. Nakatsuji, Y. Machida, Y. Maeno, T. Tayama, T. Sakakibara, J. van Duijn, L. Balicas, J. Millican, R. Macaluso, and J. Chan, Phys. Rev. lett. **96**, 087204 (2006).

[24] Y. Machida, S. Nakatsuji, H. Tonomura, T. Tayama, T. Sakakibara, J. van Duijn, C. Broholm, and Y. Maeno, J. Phys. Chem. Solid **66**, 1435 (2005).

[25] M. Udagawa, H. Ishizuka, and Y. Motome, arXiv:cond-mat/1201.0929 (2012).

[26] S. Iguchi, N. Hanasaki, M. Kinuhara, N. Takshita, C. Terakura, Y. Taguchi, H. Takagi, and Y. Tokura, Phys. Rev. Lett. **102**, 136407 (2009).

[27] H. Okabe, N. Takeshita, M. Isobe, E. Takayama-Muromachi, T. Muranaka, and J. Akimitsu, Phys. Rev. B **84**, 115127 (2011).

[28] A. B. Pippard, *Magnetoresistance in Metals* (Cambridge University Press, 1989).